Structural Engineering and Mechanics, *Vol. 69, No. 3 (2019) 317-326*
DOI: https://doi.org/10.12989/sem.2019.69.3.317

Seismic risk assessment of intake tower in Korea using updated fragility by Bayesian inference

Jahangir Alam[1a], Dookie Kim*[1] and Byounghan Choi[2b]

[1]*Civil and Environmental Engineering, Kunsan National University, 558 Daehak-ro, Gunsan-si 54150, Republic of Korea*
[2]*Rural Research Institute, 870, Haean-ro Sangnok-gu, Ansan-si Gyeonggi-do, 15634, Republic of Korea*

(Received September 15, 2018, Revised January 14, 2019, Accepted January 15, 2019)

Abstract. This research aims to assess the tight seismic risk curve of the intake tower at Geumgwang reservoir by considering the recorded historical earthquake data in the Korean Peninsula. The seismic fragility, a significant part of risk assessment, is updated by using Bayesian inference to consider the uncertainties and computational efficiency. The reservoir is one of the largest reservoirs in Korea for the supply of agricultural water. The intake tower controls the release of water from the reservoir. The seismic risk assessment of the intake tower plays an important role in the risk management of the reservoir. Site-specific seismic hazard is computed based on the four different seismic source maps of Korea. Probabilistic Seismic Hazard Analysis (PSHA) method is used to estimate the annual exceedance rate of hazard for corresponding Peak Ground Acceleration (PGA). Hazard deaggregation is shown at two customary hazard levels. Multiple dynamic analyses and a nonlinear static pushover analysis are performed for deriving fragility parameters. Thereafter, Bayesian inference with Markov Chain Monte Carlo (MCMC) is used to update the fragility parameters by integrating the results of the analyses. This study proves to reduce the uncertainties associated with fragility and risk curve, and to increase significant statistical and computational efficiency. The range of seismic risk curve of the intake tower is extracted for the reservoir site by considering four different source models and updated fragility function, which can be effectively used for the risk management and mitigation of reservoir.

Keywords: seismic risk assessment; intake tower; probabilistic seismic hazard analysis; seismic fragility, bayesian inference

1. Introduction

The Geumgwang reservoir located at 36.99ºN and 127.33ºE is one of the largest reservoirs in South Korea with water storage capacity1059ha.m. The reservoir is supplying water for the agricultural purpose of 4830ha land. The release of the water is controlled by outlet work including intake tower. The intake tower plays a significant role in preventing the catastrophic failure of reservoir dam after an earthquake, by controlling the water level and reducing the corresponding hydrostatic pressure. A cantilever freestanding high-rise tower of height 62.07 m is modeled due to its high-water level. Due to its higher height and complexity, seismic risk analysis are the crucial factors taken into consideration. Seismic risk assessment method describes the potential damages and losses due to future earthquakes and their probabilities of occurrence in a given period. FEMA (2001) developed a comprehensive earthquake loss estimation methodology which is using by the state, regional and local government for planning and earthquake loss mitigation. Multihazard Mitigation Council (2005) provided how to calculate expected annual losses including direct and indirect business interruption costs, the value of avoided statistical death and injuries and so on. The methodology for performance-based earthquake engineering and its application in seismic risk assessment was reviewed (Kalantari 2012). Many researchers studied on the seismic risk assessment of dam in Korea (Gun 2016, Ha *et al.* 2016, Alam *et al.* 2017a). However, limited guidance is available for especially assessing the seismic risk of intake tower.

The seismic fragility of the structural system is the pivotal component of seismic risk assessment, which expresses the relationship between a ground motion intensity and the corresponding probability of failure in a specific performance criterion. The lognormal model is the commonly used method for calculating the structural fragility. Kennedy *et al.* (1980) was the first who present a detailed procedure for the estimation of median ground acceleration capacity. Shinouzuka *et al.* (2000) proposed the maximum likelihood estimation method to calculate the fragility parameter. An approximate approach to evaluate the seismic fragility curves for frame structures was developed based on the statistical characteristics of peak story drifts of frame structures during earthquakes (Lin 2008). Seismic fragility of a high-rise telecommunication tower was investigated using the endurance time analysis (ETA) method (Hariri-Ardebili *et al.* 2014). Mehani *et al.* (2013) developed a framework for seismic fragility analysis

*Corresponding author, Professor
E-mail: kim2kie@kunsan.ac.kr
[a]Graduate student
E-mail: mja31.ruet@gmail.com
[b]Ph.D
E-mail: han1020@gmail.com

http://www.techno-press.com/journals/sem&subpage=7
ISSN: 1225-4568 (Print), 1598-6217 (Online)

of existing RC structure based on the post-earthquake recorded damage data. Moreover, the system fragility analysis approach was investigated for the purpose of risk management of critical facilities like piping system (Ju *et al.* 2013). The Incremental Dynamic Analysis (IDA) was used for performing a comprehensive assessment of the behavior of structure under seismic load (Vamvatsikos and Cornell 2002). The fragility parameters using these direct statistical methods require a large number of numerical analyses data which is not computationally efficient. The Bayesian inference method is used in this research for updating the fragility parameters from prior information. This method is a powerful tool for updating fragility parameters when new information becomes available. Many researchers used Bayesian inference method for estimating fragility parameters. Pei and Van de Lindt (2009) applied Bayesian approach to update and develop the probabilistic capacity and demand model using experimental data of wood frame structure. Koursourelakis (2010) suggested a Bayesian framework considering four different ground motion intensity measure to calculate fragility parameters and applied it in geotechnical field. A Bayesian approach was illustrated for seismic collapse risk assessment on a four-story reinforced concrete moment frame building (Gokkaya *et al.* 2015). Alam *et al.* (2017b) applied Bayesian inference technique for the fragility analysis of intake tower. Most of these research works have a common theme, like estimating the seismic fragility by integrating the numerical analysis or different test results.

In this study, total 30-time history analyses and a nonlinear static pushover analysis have been performed of the intake tower. Then conventional lognormal approach is used for constructing fragility curve from the both numerical analysis data. Afterward, the Bayesian inference method is used to update the fragility parameters by integrating both analyses data with the help of MCMC simulation. PSHA method is used to determine seismic hazard of the reservoir site. Four different seismic source models of Korea are considered for the hazard analysis which is developed based on historical and instrumental earthquake catalog (Choi *et al.* 2009). Also, the most probable earthquake scenario of the reservoir site is shown by hazard deaggregation. Finally, the seismic risk curve of intake tower is developed by the convolution of updated fragility and hazard function.

2. Seismic risk assessment

Seismic risk assessment is used mostly to quantify the potential damages loss due to future earthquakes and their probabilities of occurrence in a given period (Brabhaharan *et al.* 2005). Sometimes it is very essential for earthquake engineers to know the probability that loss will exceed a particular value during a given time t as a function of loss. In this research, the lognormally distributed loss measure method is used for estimating the risk curve of single structure (Porter 2016). The risk curve of the intake tower is expressed as the percentage of the probable loss (FEMA 2001, Kalantari 2012, Farsangi 2014). Seismic risk curve can be calculated by integrating the seismic hazard function and seismic fragility function with respect to the ground motion intensity.

$$R(y) = \int_{=0}^{\infty} -(1 - P(Y \leq y|IM = x))\frac{dG(x)}{dx}dx \qquad (1)$$

where Y is the uncertain degree of loss, x is a particular value of the ground motion intensity, $R(y)$ annual frequency with which loss of degree y is exceeded, $G(x)$ is the mean annual frequency of shaking exceeding intensity x and $P(Y \leq y|IM = x)$ is the cumulative distribution function of IM evaluated at y for given shaking x. Risk curve can be estimated by numerically integrating of the n discrete values of earthquake intensity x (Porter 2016).

$$R(y) = \sum_{i=1}^{n}\left(p_{i-1}(y)a_i - \frac{\Delta p_i(x)}{\Delta s_i}G_{i-1}\left(\exp(m_i\Delta s_i)\left(\Delta s_i - \frac{1}{m_i}\right) + \frac{1}{m_i}\right)\right) \qquad (2)$$

where

$$a_i = G_{i-1}(1 - \exp(m_i\Delta s_i))$$

$$p_i(y) = P(Y \leq y|IM = x) = 1 - \phi\left(\frac{\ln\left(\frac{y}{\theta(x_i)}\right)}{\beta(x_i)}\right)$$

$$m_i = \frac{\ln\frac{G_i}{G_{i-1}}}{\Delta s_i} \text{ for } i = 1,2,\dots\dots n$$

3. Seismic structural fragility

Seismic structural fragility defines as the probability of failure, that the seismic demand placed on the structure (D) is greater than the capacity of structure (C). The governing mathematical expression is as follows

$$\mathrm{G}(C, D) = C - D \qquad (3)$$

where damage gate $\mathrm{G}(C, D)$ is a function of at least two variables representing various experimental, material, modeling and loading uncertainties for the structure. The probability statement is controlled by a selected intensity measure (IM) parameter represents the seismic loading (Tadinada 2012).

$$\text{Seismic fragility} = P[D \geq C|IM] = P[C - D \leq 0|IM] \qquad (4)$$

The capacity C also called strength of a structure can be defined as the maximum seismic load that the structure can resist without occurring any damage. The capacity is assumed to be deterministic. The fragility of structure is assumed to follow some probability distribution function which is identified from both damage state and ground motion intensity.

$$P[D \geq C|IM] = F_{ij}(C_i) \tag{5}$$

where F_{ij} expresses the cumulative distribution function. Lognormal distribution is commonly used to represent the collapse fragility curve (Bradley 2008, Baker 2013) and is used in this study.

$$P(C|IM) = F_{ij}(C_i) = \phi\left(\frac{\ln IM - \ln x_m}{\beta}\right) \tag{6}$$

where $F_{ij}(C_i)$ denotes the fragility function for ground motion IM, $\phi()$ denotes the standard normal cumulative distribution function(CDF), x_m is the median value of the distribution function, and β denotes the logarithmic standard deviation or dispersion of $\ln IM$.

3.1 Incremental dynamic analysis (IDA)

There are different methods for estimating the two main parameters x_m and β of fragility curve based on lognormal model. IDA is a method of determining fragility parameters that is utilized to estimate the seismic performance of structural systems. IDA method involves scaling each ground motion in a suite until it causes collapse of the structure ((Vamvatsikos and Cornell 2002). The intensity measure of the ground motion is gradually increased and applied into the structural model until the collapse is occurred for lateral displacement.

Fragility parameters can be estimated from analyses data by taking logarithms of each ground motion's IM value associated with onset of collapse and computing there mean and standard deviation (Ibarra and Krawinkler 2005). Let, M be the number of specimen tested to failure, i is the index of specimen $(i = 1,2,\ldots..M)$ and IM is the value associated with the beginning of collapse for the ith ground motion (Ang and Tang 2006).

$$x_m = exp\left(\frac{1}{M}\sum_{i=1}^{M} lnIM_i\right) \tag{7}$$

$$\beta = \sqrt{\frac{1}{M-1}\sum_{i=1}^{M}\left(ln\frac{IM_i}{x_m}\right)^2} \tag{8}$$

The fragility parameters are updated and fitted by using IDA with the help of Bayesian inference and MCMC simulation.

3.2 Bayesian inference

The structural fragility model $P(C/IM)$ depends on a vector of random variable θ_i. The prior relative likelihood and joint density function can be expressed as $p_i = P(\Theta = \theta_i)$ and $f'_\Theta(\theta_1, \theta_2, ..)$. The prior information is generally available from experimental studies, professional knowledge of expert, past studies etc. (Tadinada 2012). The prior information may be updated formally through the Bayes theorem using additional observed data $(f''_\Theta(\theta_1, \theta_2, ..|Y))$ (Ang and Tang 2006, Box and Tiao 1973).

$$f''_\theta(\theta_1, \theta_2, ..|Y) = \frac{P(\theta_1, \theta_2, ..|Y) f'_\theta(\theta_1, \theta_2, ..)}{P(Y)} \tag{9}$$

$$P(Y) = E(\theta_i|Y) = \int P(\theta_1, \theta_2, ..|Y)\, f'_\Theta(\theta_1, \theta_2, ..) d\theta_i \tag{10}$$

where $P(\theta_1, \theta_2, ..|Y)$ is referred to as the likelihood function of the random parameter.

3.3 Markov chain monte carlo (MCMC)

The posterior distribution $f''_\Theta(\theta_1, \theta_2, ..|Y)$ are accounted by numerically generating a large number of sample from probability distribution using a special class of computational algorithms called Markov Chain Monte Carlo (Brooks 1998). There are several standard methods available for designing Markov chain with required stationary distribution $P(\theta|Y)$. Gibbs sampling is a special case of the Metropolis-Hastings algorithm which generates a Markov chain by sampling from full conditional distribution (Casella and George 1992). Let us assume a vector θ consist of k sub-components, $\theta = (\theta_1, \theta_2, \ldots, \theta_k)$.

Step 1 Choose starting values $\theta_1^{(0)}, \theta_2^{(0)}, \ldots\ldots\ldots \theta_k^{(0)}$

Step 2 Sample $\theta_1^{(1)}$ from $P\left(\theta_1|\theta_2^{(0)}, \theta_3^{(0)} \ldots\ldots\ldots \theta_k^{(0)}, Y\right)$

Sample $\theta_2^{(1)}$ from $P\left(\theta_2|\theta_1^{(1)}, \theta_3^{(0)} \ldots\ldots\ldots \theta_k^{(0)}, Y\right)$

……………..

Sample $\theta_k^{(1)}$ from $P\left(\theta_k|\theta_1^{(1)}, \theta_2^{(1)} \ldots\ldots\ldots \theta_{k-1}^{(1)}, Y\right)$

Eventually, we can obtain the posterior distribution sample from $P(\theta|\mathrm{Y})$ by repeating the step 2 many times. MCMC simulation method enabled quantitative researchers to use highly complicated model and estimate the corresponding posterior distribution with accuracy (Ntzoufras 2009).

4. Probabilistic seismic hazard analysis (PSHA)

To assess the seismic risk of any structure, the estimation of the annual probability or rate of exceedance of ground motion intensity for a specific site is a crucial factor for the earthquake engineer. PSHA aims to estimate the seismic hazard corresponding specific ground motion and to quantify the uncertainty about the location, size and resulting shaking intensity of future earthquakes.

4.1 Seismic source map

Korea is known as a low and moderate seismicity zone because of no strong earthquake record was measured. In addition, no active faults were identified in Korea.

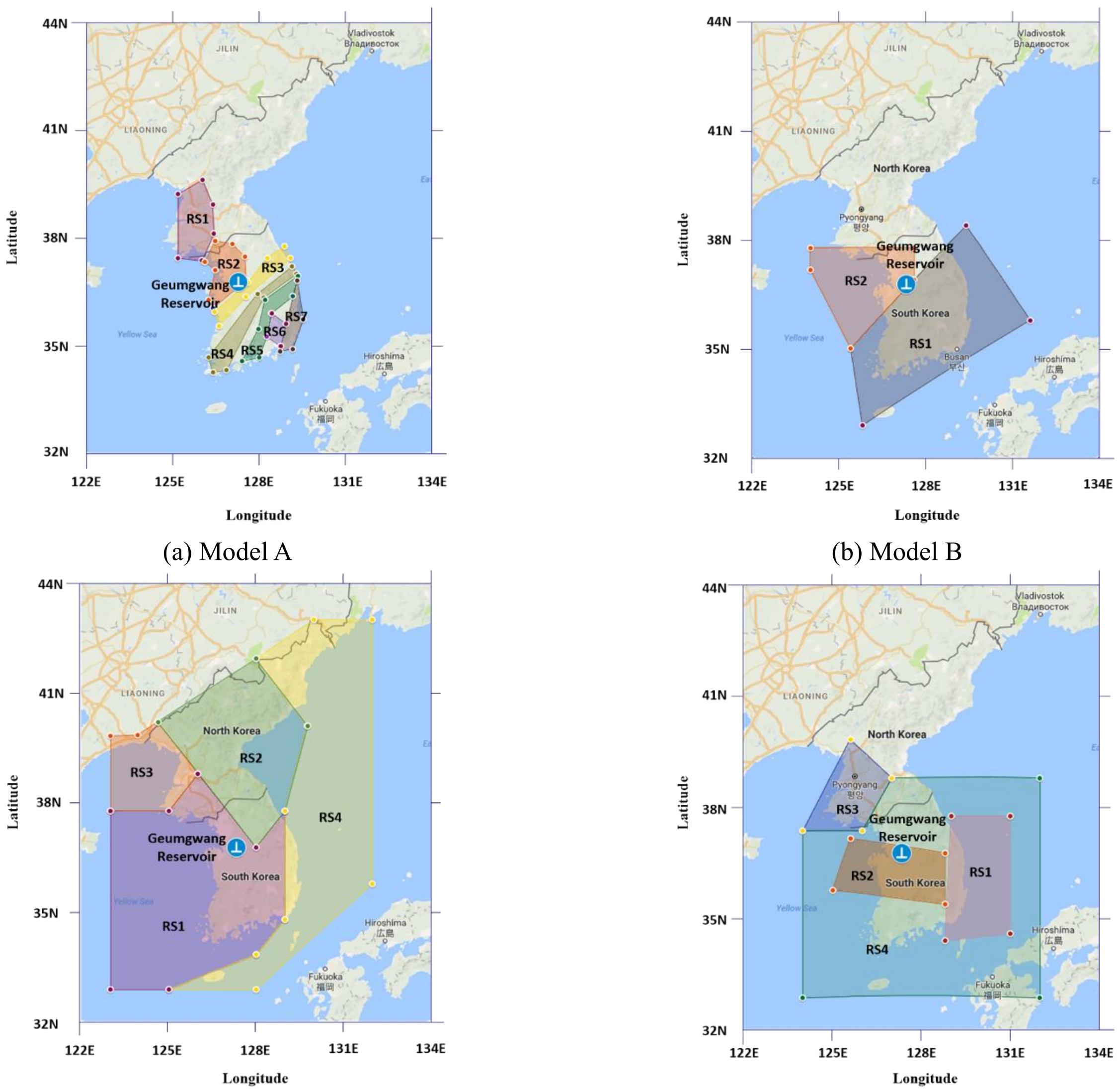

(a) Model A (b) Model B

(c) Model C (d) Model D

Fig. 1 Seismic source models of Korea for seismic hazard analysis

Therefore, the Poisson type PSHA method is used in Korea, in which all the earthquakes are presumed to occur according to a stationary process in the time domain (Choi *et al.* 2005). Recently, the seismicity expert teams proposed the four seismic source maps for the PSHA. Most of the seismic source map was proposed by using a historical and instrumental earthquake data without a distinct seismo tectonic environment. More than 2000 earthquake data were used for development the seismic source model, in which more than 1800 earthquake data had been taken from the historical earthquake records (Seo *et al.* 1999). Fig.1 shows the four-seismic source model of Korea that is used in this study (Choi *et al.* 2009). In each source area, the distribution of the earthquake size was assumed to follow the Gutenberg-Richter recurrence law and the hypocenters were assumed to be distributed uniformly and randomly (Gutenberg and Richter 1944). Table 1 shows the seismicity parameters for the four-seismic source model provided by CRIEPI32.

4.2 Overview of PSHA

The probability of exceedance of a particular value of x of ground motion parameter (IM) can be calculated by multiplying the probability of specific earthquake magnitude that would occur at a particular location to the probability of one possible earthquake and one possible location of source. The process is then repeated for all possible earthquake magnitude and sources and summed (Baker 2015, Kramer 1966). In general, PSHA can consider the aleatory uncertainties of earthquake magnitude (M), source to site distance (R) and wave attenuation. The governing equation is as follows (McGuire 1976)

$$\lambda(IM > x) = \sum_{i=1}^{N_S} v_i \sum_{j=1}^{N_M} \sum_{k=1}^{N_R} P(IM > x | m_j, r_k) P(M_i = m_j) P(R_i = r_k) \tag{11}$$

where N_s, N_M and N_R are the number of potential

Table 1 Seismicity parameters for the seismic source models

Source model	Source ID	Seismicity parameters a	Seismicity parameters b	Max. Magnitude	Min. Magnitude
Model A	RS1	4.28	1.12	6.6	3.8
	RS2	3.53	0.92	6.9	
	RS3	2.59	0.69	7.1	
	RS4	2.34	0.66	6.7	
	RS5	3.10	0.87	7.1	
	RS6	2.12	0.66	6.7	
	RS7	1.70	0.59	7.2	
Model B	RS1	2.93	0.76	6.7	3.0
	RS2	2.53	0.75	6.5	
Model C	RS1	3.09	0.8	6.3	3.5
	RS2	2.98	0.8	6.3	
	RS3	2.51	0.7	7.0	
	RS4	1.55	0.6	6.5	
Model D	RS1	1.09	0.58	7.0	3.0
	RS2	1.97	0.58	6.8	
	RS3	2.58	0.58	6.8	
	RS4	2.29	0.58	6.5	

earthquake sources, different earthquake magnitudes and different source to site distances respectively; $P(IM > x)$ is the probability that a ground motion parameter (IM) will exceed a particular value of x (Baker 2015, Kramer 1966).

$$P(IM > x) = \int_{m_{min}}^{m_{max}} \int_{0}^{r_{max}} P(IM > x|m_j, r_k) f_M(m) f_R(r)\, dr\, dm \quad (12)$$

where $f_M(m)$ and $f_R(r)$ are the probability density function for magnitude and distance respectively and $P(IM > x|m_j, r_k)$ comes from ground motion model. ν_i from Eq. (11), commonly express as the annual rate of earthquake occurrence, governed by Gutenberg and Richter (1944) as follows

$$\nu_i = 10^{a-bm_i} \quad (13)$$

where a and b values are known as the Gutenberg - Richter recurrence parameters. The resulting probability distribution of magnitude for the Gutenberg-Richter law can be determined by the ratio between the number of earthquake in a magnitude range prescribed to the total number of earthquakes (McGuire and Arabasz 1990).

$$P(m_1 \le M < m_2 | m_0 \le m_1, m_2 \le m_{max}) = \frac{10^{-bm_1} - 10^{-bm_2}}{10^{-bm_0} - 10^{-bm_{max}}} \quad (14)$$

where m_0 and m_{max} are the lower threshold magnitude and maximum magnitude. Therefore, the seismicity parameters (a, b, m_0, m_{max}) of each source model are pivotal part for probabilistic seismic hazard analysis (Wang *et al.* 2013). The accuracy of the numerical integration of Eq. (11) can be increased with the increasing of number of magnitude (N_M) and distance (N_R).

4.3 Ground motion model

Ground motion prediction model are generally developed using statistical regression of observed ground motion intensities. To describe the probability distribution function, prediction models consider the following general form (Baker 2015).

$$\ln IM = \overline{\ln IM}(M, R, \theta) + \sigma(M, R, \theta).\varepsilon \quad (15)$$

where the terms $\overline{\ln IM}(M, R, \theta)$ and $\sigma(M, R, \theta)$ are the predictive mean and standard deviation respectively and which are the output of the ground motion prediction model. Over decades of development and refinement, many prediction models for the term $\overline{\ln IM}(M, R, \theta)$ and $\sigma(M, R, \theta)$ have been developed consisting many terms and tables containing a number of coefficient. In this paper, predictive model of Cornell *et al.* (1979) is used for the mean of log peak ground acceleration (in units of g).

$$\overline{\ln PGA} = -0.152 + 0.859M - 1.803\ln(R + 25) \quad (16)$$

The standard deviation of $\ln PGA$ is 0.57 in this model which is constant for all magnitudes and distances.

4.4 Hazard deaggregation

The seismic hazard analysis expresses the mean annual rate of exceedance for particular ground motion intensity at any specific site base on the different source and their magnitudes and distances. In some cases, it is very supportive to account the most likelihood earthquake magnitudes and the most likely source to site distance, which is contributing to maximum hazard for a particular ground motion parameter. The deaggregtion process reveals the mean annual rate of exceedance as a function of magnitude and distance (Baker 2015, Kramer 1966).

$$\lambda(IM > x, M = m, R = r) = P(M_i = m)P(R_i = r \sum_{i=1}^{N_S} \nu_i P(IM > x|m_j, r_k) \quad (17)$$

5. Structural analysis of intake tower

In this research, the seismic risk assessment of high rise free standing intake tower is analyzed. The numerical analysis of intake tower is conducted by considering the lumped mass model in OpenSees.

5.1 Tower geometry

The details elevation of cantilever free standing intake

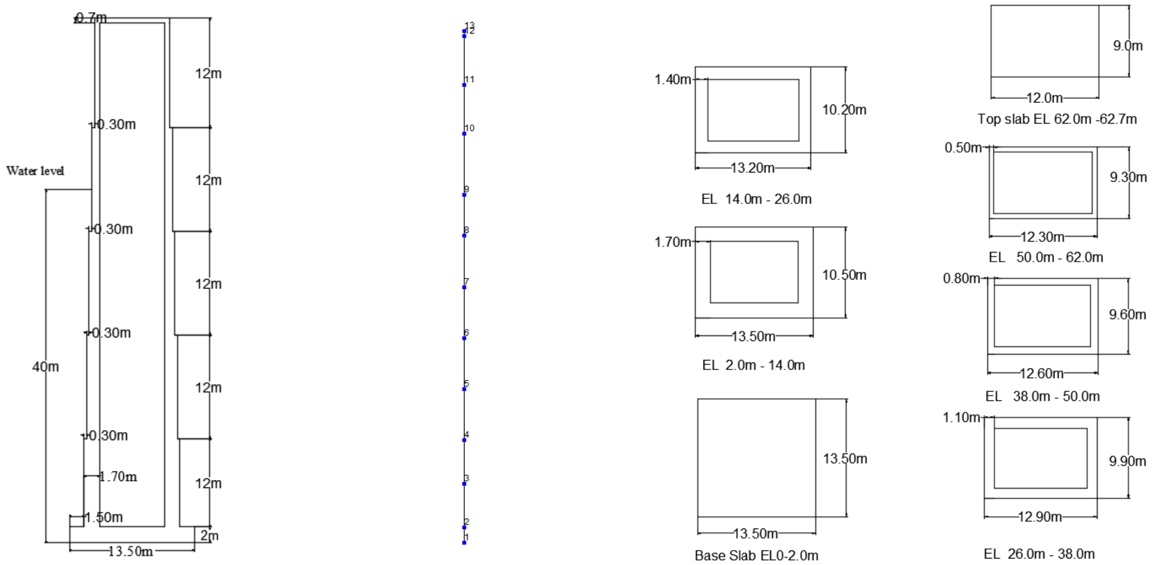

(a) Elevation (b) lumped-mass model (c) Typical section and dimension of intake tower

Fig. 2 Details of intake tower model

tower of height 62.7 0m is shown in Fig. 2(a). The cross-sections of the tower are rectangular which varies from (13.50 m × 13.50 m) at the base to (12.0 m × 11.0 m) at the top as shown in Fig. 2(c). Moreover, the thickness of the tower differs from section to section. The thickness of the tower is 1.70 m and 0.70 m at the bottom and top section respectively. The tower has a 2.0 m deep concrete slab at the bottom and 0.70 m deep concrete slab at the top of the tower.

5.2 Hydrodynamic masses

The refine method (USACE 2003) is used to calculate the inside and outside hydrodynamic masses of the intake tower. In short, this method is carried out by converting each uniform section of the tower, first into an equivalent uniform elliptical section and then into a corresponding equivalent circular section. The normalized hydrodynamic added mass $m_{\infty}^{0}/\rho_w A_0$ due to outside water is calculated from the width to depth ratio of the average cross-section. Finally, the absolute added hydrodynamic mass can be calculated by multiplying $\rho_w A_0$ with the normalized added mass, where ρ_w and A_0 are the water mass density and outside area of the average section.

5.3 Failure identification

According to USACE guidance document, a displacement based dynamic analysis may be used to identify the failure of the intake tower. If the displacement demand (δ_D)at the top of the tower surpass the ultimate displacement capacity (δ_u) is considered as the failure criteria. The maximum top deflection of the tower named as the displacement demand estimated using time history analysis with linear spring properties, beam column elements properties and added hydrodynamic mass due to circumambient or contained water. The ultimate displacement capacity at the top of the tower is allied to the height of the tower, the width of the plastic hinge and the fracture strain capacity.

$$\delta_u = \frac{\emptyset_E l^2}{3} + \theta_p l^2 \tag{18}$$

$$\delta_u \emptyset_E = \frac{M}{EI_g} \tag{19}$$

where δ_u is the ultimate displacement capacity, $\emptyset_E$ = the elastic curvature at cracking (at the base of the tower), $\emptyset_p$ is the plastic rotation at failure, M is the moment at the base of the tower and $l =$ the height of the tower above the crack. The ultimate deflection capacities at the top of the tower are calculated as 10.1 cm and 12.8 cm about the strong axis and weak axis, respectively.

6. Results and discussion

The Bayesian inference with MCMC simulation is used to update the seismic fragility from prior information. Prior information is usually estimated from the existing studies of similar structure, professional experience or any simplified analysis method. In this study, nonlinear static pushover analysis and 30 number of time history analyses are performed as prior information.

The nonlinear static pushover analysis is used in this study, because the analysis is generally performed before the dynamic analysis and is not computationally demanding. Vamvatsikos and Cornell (2005) provided a fast and accurate method named SPO2IDA to estimate the seismic demand and capacity. The method makes the connection between the Static Pushover (SPO) and the

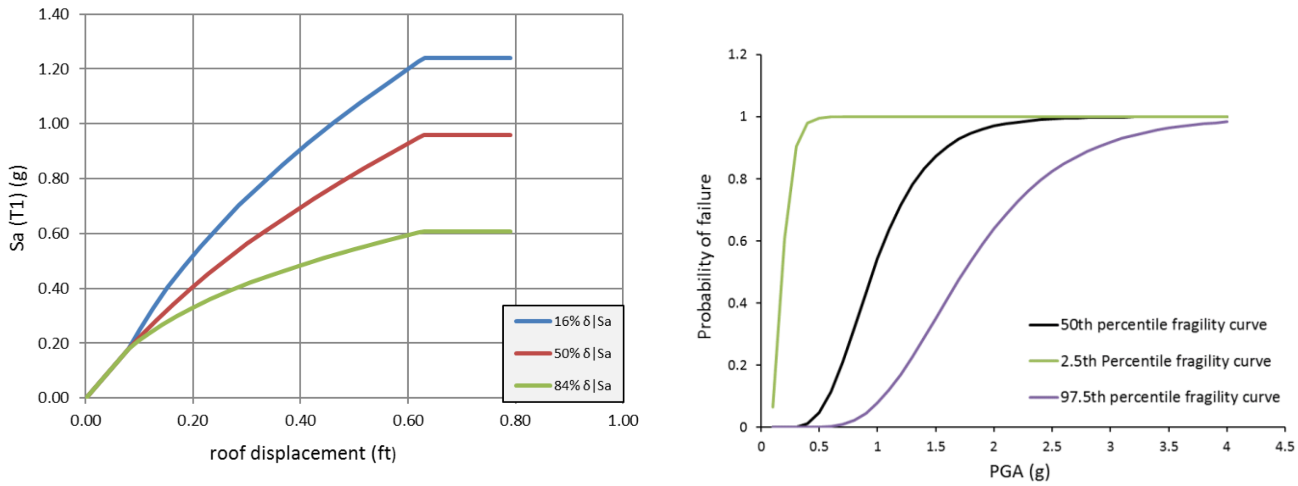

(a) 16, 50 and 84% fractal IDA curves (b) 95% confidence bound of fragility curves

Fig. 3 Lognormal fragility curves with 95% confidence interval from pushover analysis using SPO2IDA software by Vamvatsikos and Cornell (2005)

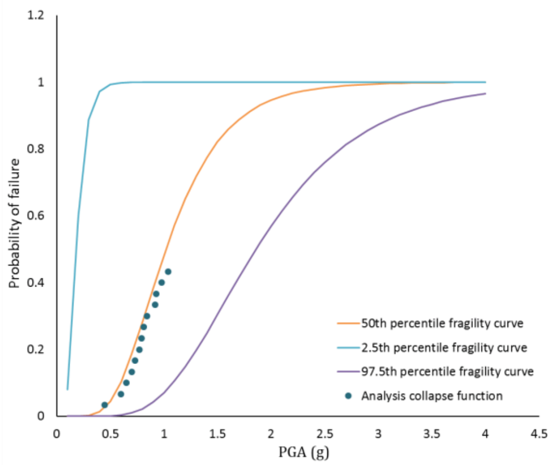

Fig. 4 Lognormal fragility curve with 95% confidence band region using from 30-time history analyses

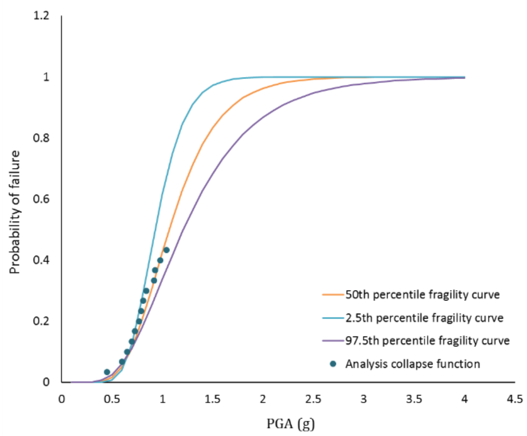

Fig. 5 Updated fragility curve with 95% confidence interval using Bayesian inference and MCMC simulation

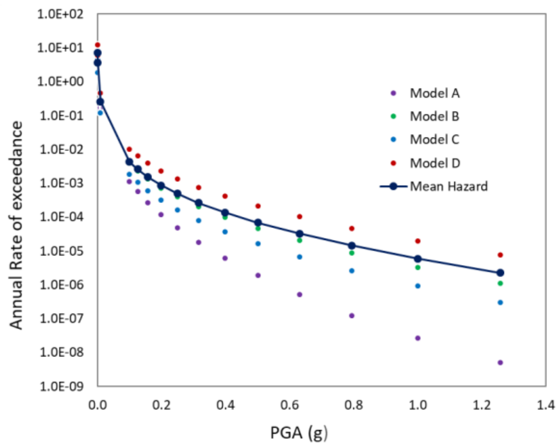

Fig. 6 PGA seismic hazard curve at the Geumgwang reservoir located at 36.990N and 127.330E for four seismic source models of Korea

Incremental Dynamic Analysis (IDA) and infers nonlinear dynamic response using pushover analysis result. 16, 50 and 84% fractal IDA curves are obtained using SPO2IDA method from the data of static pushover analysis as shown in Fig. 3(a). This IDA curves lead to lognormal fragility function having median collapse capacity 0.96g and dispersion of 0.39. Fig. 3(b) illustrates the 95% confidence bound of median fragility curve using the fragility parameters mention above.

In case of IDA, fragility parameters are calculated by taking logarithms of each ground motion associated with onset of collapse. Thirty number of time history analyses are performed on the intake tower model and among them 13 number of collapses are experienced on the basis top tower displacement limit measure. Lognormal fragility parameters having median collapse parameter 1.02 g and dispersion 0.42 are calculated using the collapse number. Fig. 4 describes the fragility curve with 95% confidence bound using IDA methods.

The fragility curves from both analyses are noticed the wide confidence interval which indicate large uncertainty of

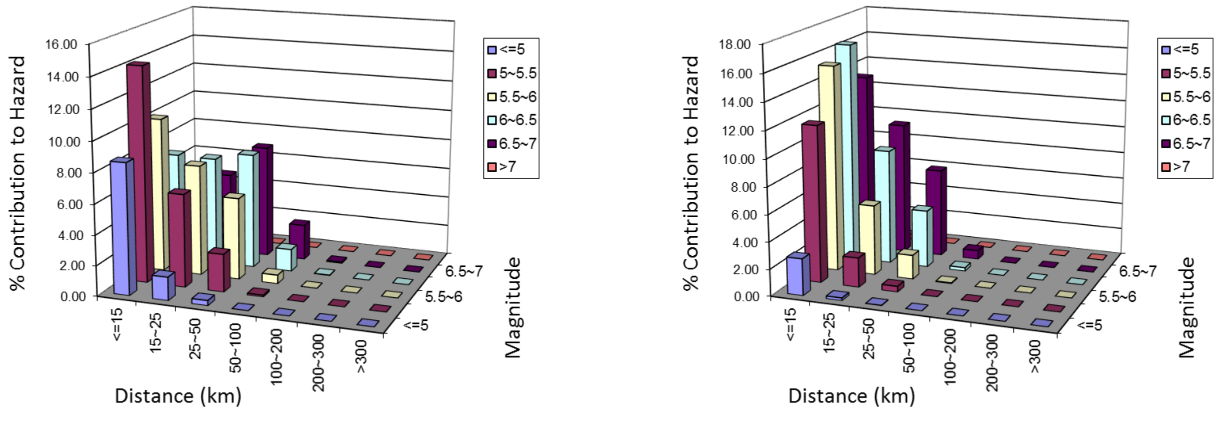

(a) (b)

Fig. 7 Hazard deaggregation for Geumgwang reservoir at two customary hazard levels: (a) 10% exceedance probability in 50 years, and (b) 2% exceedance probability in 50 years

the median fragility curve. A large number of additional data is required for reducing the uncertainty using these conventional fragility model which increase the computational time and cost. Bayesian inference is employed for integrating data from static pushover analysis and time history analysis with the help of MCMC simulation. Fig. 5 illustrates the 95% confidence band of median fragility curve using Bayesian Inference and MCMC simulation which express the reduction of uncertainty of median fragility curve.

The seismic hazard curves are developed using the four-seismic source model of Korea. Fig. 6 shows the seismic hazard curve for PGA as ground motion intensity measure at the Geumgwang reservoir site for the four-seismic source model. From the hazard curve, we can see that the annual rate of exceedance for model D is higher than any other sources which means the highest hazard contribution is from source model D. It is because the source model D includes some earthquake record data from far sources i.e., some part of Japan and Yellow sea. A mean seismic hazard curve is extracted due its variation of exceedance rate for different sources model and to consider the uncertainty of the source model (Fig. 6).

Hazard deaggregation are generally estimated for six default hazard rates as follows: 0.1, 0.01, 0.0021, 0.001, 0.0004 and 0.0001 (Wang *et al.* 2013). The annual rate of 0.0021 and 0.0004 are the two customary hazard levels equivalent to 10% and 2% exceedance probabilities within in 50 years for Poisson process recommended by Kramer (1966), which are used for this study. Fig. 7 shows the respective PGA hazard deaggregation at the two hazard levels for the highest contribution hazard source model D. Seismic source model D is considered for hazard deaggregation because of the higher hazard rate. From Fig. 7, it is found that 90% of hazard are contributed by magnitudes (5.0-6.5M_w) occurring relatively close to the site (i.e., 0-50 km).

The seismic risk curves, as shown in Fig. 8 are calculated by integrating the seismic hazard probability and

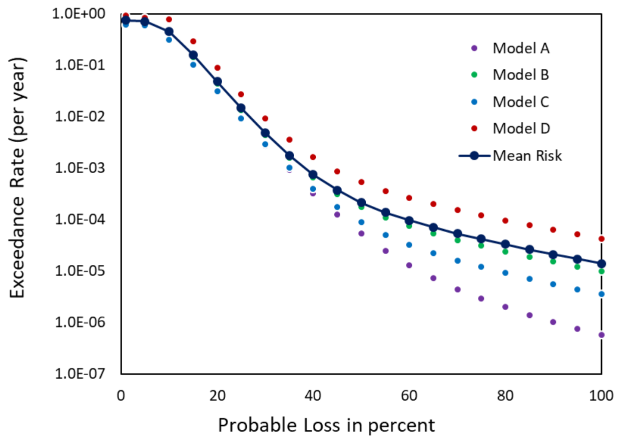

Fig. 8 Seismic risk curve of intake tower at the Geumgwang reservoir for four different source models

the updated fragility function corresponding to similar intensities. The mean seismic risk curve of intake tower as shown in figure is recommended for reservoir site to decrease the source model uncertainty due to the variation of hazard rate for different source model. From Fig. 8, we can easily predict the future loss of the structure due to earthquake hazard corresponding design service life. It also illustrates the life cycle cost that can be used in the life cycle management and maintenance of the structural system.

6. Conclusions

The focus of this study is to quantify the seismic risk of the intake tower at Geumgwang reservoir in Korea for managing the risk associated with the reservoir. The seismic risk of the intake tower is assessed by updating the fragility functions using Bayesian inference and MCMC simulation. The method provides a worthy way to embody the different types of risk data and to update the fragility parameters when new information become available. Seismic hazard is analyzed by using the PSHA method for four different seismic source models of Korea. The hazard deaggregation has been performed at two customary hazard levels to show the hazard contribution for different earthquake magnitude and distance. The mean hazard curve is extracted for the risk assessment due to the variation of the hazard curve for different sources. The uncertainty associated with the median fragility curve for both static pushover analysis and dynamic analysis is shown by the 95 percent confidence bound. The confidence bound associated with each fragility curves appears quite wide indicating large uncertainties. Updating fragility curve obtaining from combining the analysis results by Bayesian inference shows the significant reduction of uncertainty of the 95 percent confidence band region. The mean risk curve of intake tower is suggested for the reservoir site which can play a significant role for risk management and mitigation of reservoir system.

Acknowledgments

This research was supported by a grant(2017-MOIS31-002) from Fundamental Technology Development Program for Extreme Disaster Response funded by Korean Ministry of Interior and Safety (MOIS).

References

Alam, J., Kim, D. and Choi, B. (2017a), "Seismic probabilistic risk assessment of weir structures considering the earthquake hazard in the Korean Peninsula", *Earthq. Struct.*, **13**(4), 421-427.

Alam, J., Kim, D. and Choi, B. (2017b), "Uncertainty reduction of fragility curve of intake tower using bayesian inference and markov chain monte carlo simulation", *Struct. Eng. Mech.*, **63**(1), 47-53.

Ang, A.H.S. and Tang, W.H. (2006), *Probability Concepts in Engineering*, Vol. I, John Wiley & Sons, New York, U.S.A.

Baker, J.W. (2015), *Probabilistic Seismic Hazard Analysis*, White Paper Version 2.0.1.

Baker, J.W. (2013), "Efficient analytical fragility function fitting using dynamic structural analysis", *Earthq. Spectr.*, **31**(1), 579-599.

Box, G.E.P. and Tiao, G.C. (1973), *Bayesian Inference in Statistical Analysis*, Wiley, ISBN 0-471-57428-7.

Brabhaharan, P., Davey, R., O'Riley, F. and Wiles, L. (2005), *Earthquake Risk Assessment Study Part 1-Review of Risk Assessment Methodologies and Development of a Draft Risk Assessment Methodology for Christchurch*, Report No SPT 2004/28.

Bradley, B.A. and Dhakal, R.P. (2008), "Error estimation of closed-form solution for annual rate of structural collapse", *Earthq. Eng. Struct. Dyn.*, **37**(15), 1721-1737.

Brooks, S.P. (1998), *Markov Chain Monte Carlo Method and Its Application*, The Statistician, **47**, 69-100.

Casella, G. and George, E.I. (1992), "Explaining the gibbs sampler", *Am. Statistic.*, **46**(3), 167-174.

Choi, I.K., Nakajima, M., Choun, Y.S. and Ohtori, Y. (2005), *Evaluation of the Current Seismic Zone of Korea Based on the Probabilistic Seismic Hazard Analysis*, KNS Spring Meeting.

Choi, I.K., Nakajima, M., Choun, Y.S. and Ohtori, Y. (2009), "Development of the site-specific uniform hazard spectra for Korean nuclear power plant sites", *Nucl. Eng. Des.*, **239**(4), 790-799.

Cornell, C.A., Banon, H. and Shakal, A.F. (1979), "Seismic motion and response prediction alternatives", *Earthq. Eng. Struct. Dyn.*, **7**(4), 295-315.

Farsangi, E.N., Rezvani, F.H., Talebi, M. and Hashemi, S.A.H. (2014), "Seismic risk analysis of steel-MRFs by means of fragility curves in high seismic zones", *Adv. Struct. Eng.*, **17**(9), 1227-1240.

FEMA (2001), *Earthquake Loss Estimation Methodology*, HAZUS99, Service Release 2, Technical Manual. Federal Emergency Management Agency, Washington DC, U.S.A.

Gokkaya, B.U., Baker, J.W. and Deierlein, G. (2015), "Illustrating a Bayesian approach to seismic collapse risk", *Proceedings of the 12th International Conference on Application of Statistics and Probability in Civil Engineering*, Vancouver, Canada, July.

Gun, H. (2016), "Schematic development of risk analysis for dam safety", *J. Kor. Soc. Agricult. Eng.*, **58**(2), 11-20.

Gutenberg, B. and Richter, C.F. (1944), "Frequency of earthquakes in California", *Bullet. Seismol. Soc. Am.*, **34**(4), 1985-1988.

Ha, I.S., Lee, S.G., Lim J.Y. and Jung, Y.H. (2016), "Seismic failure probability of the Korean disaster Risk fill dams estimated by considering freeboard only", *J. Kor. Soci. Civil Eng.*, **36**(3), 451-461.

Hariri-Ardebili, M.A., Rahmani-Samani, H. and Mirtaheri, M. (2014), "Seismic stability assessment of a high-rise concrete tower utilizing endurance time analysis", *Int. J. Str. Stab. Dyn.*, **14**(6), 1450016.

Ibarra, L.F. and Krawinkler, H. (2005), *Global Collapse of Frame Structures under Seismic Excitations*, Report No. 152, John A. Blume Earthquake Engineering Center, Stanford, CA, 324.

Ju, B.S., Jung, W.Y. and Hee, Y. (2013), "Seismic fragility evaluation of piping system installed in critical structures", *Struct. Eng. Mech.*, **46**(3), 337-352.

Kalantari, A. (2012*), Seismic Risk of Structures and the Economic Issues of Earthquakes*, Earthquake Engineering, InTech.

Kennedy, R.P., Cornell, C.A., Campbell, R.D., Kaplan, S. and Perla, H.F. (1980), "Probabilistic seismic safety of an existing nuclear power plant", *Nucl. Eng. Des.*, **59**(2), 315-338.

Koutsourelakis, P.S. (2010), "Assessing structural Vulnerability against earthquake using multi-dimensional fragility surface: A Bayesian framework", *Probab. Eng. Mech.*, **25**(1), 49-60.

Kramer, S.L. (1996), *Geotechnical Earthquake Engineering*, Prentice Hall Inc., New Jersey, U.S.A.

Lin, J.H. (2008), "Seismic fragility analysis of frame structures", *Int. J. Str. Stab. Dyn.*, **8**(3), 451-463.

McGuire, R.K. (1976), *FORTRAN Computer Program for Seismic Risk Analysis*, US Geological Survey, Open-File Report 76, 67.

McGuire, R.K. and Arabasz, W.J. (1990), "An introduction to probabilistic seismic hazard analysis", *Geotech. Environ. Geophys.*, **1**, 333-353.

Mehani, Y., Bechtoula, H., Kibboua, A. and Naili, M. (2013), "Assessment of seismic fragility curves for existing RC buildings in Algiers after the 2003 Boumerdes earthquake", *Struct. Eng. Mech.*, **46**(6), 791-808.

Multihazard Mitigation Council (2005), *Natural Hazard Mitigation Saves: An Independent Study to Assess the Future Savings from Mitigation Activities*, National Institute of Building Sciences, Washington, DC, U.S.A.

Ntzoufras, I. (2009), *Bayesian Modeling using WinBUGS*, John Wiley & Sons, Inc., Hoboken, New Jersey, U.S.A.

Pei, S. and Van de Lindt, J.W. (2009), "Methodology for long-term seismic loss estimation: An application to woodframe buildings", *Struct. Safety*, **31**(1), 31-42.

Porter, K. (2016), *A Beginner's Guide to Fragility, Vulnerability, and Risk*, University of Colorado Boulder, 92.

Seo, J.M., Min, G.S., Choun, Y.S. and Choi, I.K. (1999),

Reduction of Uncertainties in Probabilistic Seismic Hazard Analysis, KAERI/CR-65/99.
Shinozuka, M., Feng, M., Lee, J. and Naganuma, T. (2000), "Statistical analysis of fragility curves", *J. Eng. Mech.*, **126**(12), 1224-1231.
Tadinada, S.K. (2012), "A Bayesian framework for probabilistic seismic fragility assessment of structure", Ph.D. Dissertation, North Carolina State University, Raleigh, North Carolina, U.S.A.
USACE (2003), *Structural Design and Evaluation of Outlet Works*, EM 1110-2-2400, US Army Corps of Engineers.
Vamvatsikos D. and Cornell C.A. (2002), "Incremental dynamic analysis", *Earthq. Eng. Struct. Dyn.*, **31**(3), 491-514.
Vimvatsikos, D. and Cornell, C. A. (2005), "Direct estimation of seismic demand and capacity of MDOF systems through incremental dynamic analysis of an SDOF approximation", *J. Struct. Eng.*, **131**(4), 589-599
Wang, J.P., Huang, D., Cheng, C.T., Shao, K.S., Wu, Y.C. and Chang, C.W. (2013), "Seismic hazard analyses for Taipei city including deaggregation, design spectra, and time history with excel applications", *Comput. Geosci.*, **52**, 146-154.

CC